Path Planning for Reconfigurable Rovers in Planetary Exploration

C.J. Pérez-del-Pulgar[1], J.R. Sánchez[1], A.J. Sánchez[1], M. Azkarate[2] and G. Visentin[2]

***Abstract*— This paper introduces a path planning algorithm that takes into consideration different locomotion modes in a wheeled reconfigurable rover. Power consumption and traction are estimated by means of simplified dynamics models for each locomotion mode. In particular, wheel-walking and normal-driving are modeled for a planetary rover prototype. These models are then used to define the cost function of a path planning algorithm based on fast marching. It calculates the optimal path, in terms of power consumption, between two positions, providing the most appropriate locomotion mode to be used at each position. Finally, the path planning algorithm was implemented in V-REP simulation software and a Martian area was used to validate it. Results of this contribution also demonstrate how the use of these locomotion modes would reduce the power consumption for a particular area.**

I. INTRODUCTION

Planetary exploration is nowadays in the spotlight since space agencies have been preparing different missions to place rovers in other planets and satellites [1]. The aim of these rovers is to carry instruments while moving towards scientifically interesting places. Currently, the European Space Agency is organizing the ExoMars mission, whose objective is to place a rover in the Martian surface in 2020 [2]. This rover has a triple bogie suspension based on an actuated 6x6x6 DoF kinematic configuration: 6 wheel, 6 steering and 6 walking motors [3]. Due to past missions have shown the difficulties the rover may encounter traversing certain terrains such as soft soil in dunes [4], this configuration enables the rover to use a *wheel-walking* locomotion mode. It was experimentally demonstrated that improves traction in loose soil [5]. Furthermore, a similar locomotion mode, called *inching locomotion*, can be found in [6], which was also experimentally validated. In particular, they used a testbed that showed the displacement of soil during its interaction with a wheel. So, they demonstrated the source of the tractive improvement. However, while there is so much research on modeling wheel-soil interaction in *normal driving* locomotion [7], to the authors knowledge, there are no works related to *wheel-walking*. Modeling of this locomotion mode arises useful to decide whether it may be suitable for given terrain features. Moreover, this decision may be included in a particular path planning algorithm, whose aim would be the minimization of power consumption.

*This work was partially supported by the European Space Agency, under contract number 4000118072/16/NL/LvH/gp

[1]C.J. Pérez-del-Pulgar, J.R. Sánchez and A.J. Sánchez are with the Department of Automation and Systems Engineering, Universidad de Malaga, Andalucia Tech, 29070 Málaga, Spain carlosperez@uma.es

[2]M. Azkarate and G. Visentin are with the European Space Agency, ESTEC, Noorwijk, Netherlands gianfranco.visentin@esa.int

As regards this kind of path planning algorithms, E. Rohmer et al. [8] proposed a method based on two stages: first, they used the Dijkstra path planning algorithm to choose the best path; and second, they used another algorithm to choose the best locomotion mode for each point in the previously planned path. Nevertheless, this method would not be able to optimize the total cost of the planned path in terms of power consumption. The main reason is because the locomotion modes are not considered during the path planning stage.

This paper proposes two simplified dynamics models for the *normal driving* and *wheel-walking* locomotion modes, which provides information about their power consumption for different friction and slip coefficient values. The comparison is then used to define a cost function that provides the best locomotion mode and its cost. Then, it is used in a modified fast marching path planning algorithm [9], which provides the optimal and smoothest path plan, and the corresponding locomotion mode at every planned position. Finally, parameters of the ExoTeR rover [5], a triple-bogie lab rover prototype owned by the European Space Agency, have been used to setup the model parameters. Moreover, the path planning algorithm has been implemented in V-REP, using the ExoTeR rover and a Martian area within the simulation scene.

II. LOCOMOTION MODES

As previously stated, this paper studies the use of two locomotion modes to minimize power consumption: *wheel-walking* and *normal driving*. Each one provides a better performance of the rover displacement depending on terrain and rover features. Many aspects should be taken into consideration, however, the main issue is the fact that the energy available for the rover is not infinite, i.e. the power consumption of motors should be optimized. As a result, it strongly influences on the selection of the rover locomotion mode for traversing a determined path.

To calculate the power consumption for both locomotion modes, terrain features have been simplified by means of two parameters [10]: dynamic friction (μ) and slip ratio (s). The dynamic friction represents the rolling resistance, i.e. the force that is opposed to the motion of the wheels; and the slip ratio is the relation between the ground and wheel velocity, which express whether the wheel is sliding or not. These parameters are expressed as:

$$\mu = F_f / F_N \tag{1}$$

$$s = 1 - \frac{v}{rw} \tag{2}$$

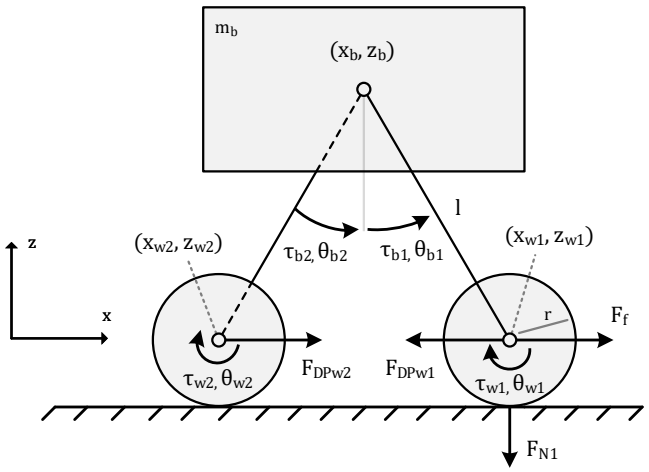

Fig. 1: Diagram of the proposed wheel-walking model where positions, forces and torques are depicted.

where F_f is the friction force, F_N is the normal force that exerts the wheel over the ground, v is the linear ground velocity of the rover, r is the wheel radius and w is the angular velocity of the wheel. Although these parameters could vary depending on the rover and terrain configuration, e.g. velocity, soil features, wheel, etc. they could be obtained through sensors and estimated using different algorithms [11]. These parameters are used to model both locomotion modes as follows.

A. Wheel-walking

The *wheel-walking* locomotion mode is represented in Figure 1 for a rover with $n = 2$ wheels, where (x_{w1}, z_{w1}) and (x_{w2}, z_{w2}) represent the position of the wheel centers, (x_b, z_b) is the center of the rover body, which coincides with the position of the walking motors, each one for each wheel. On the other hand, θ_{b1} and θ_{b2} represent the angle of rotation of the wheel leg with respect to the vertical. Relation between positions and angles of the rover body are expressed as:

$$x_b = x_{w1} - l \cdot sin(\theta_{b1}) \tag{3}$$

$$z_b = z_{w1} + l \cdot cos(\theta_{b1}) \tag{4}$$

On the other hand, each wheel rotates an angle θ_{w1} and θ_{w2}. Position of the center of the first wheel (x_{w1}, z_{w1}) is used as the reference; and position of the second wheel is defined as:

$$x_{w2} = x_b - l \cdot sin(\theta_{b2}) \tag{5}$$

$$z_{w2} = z_b - l \cdot cos(\theta_{b2}) \tag{6}$$

To improve the explanation of this locomotion mode, dynamics of each actuated joint will be separately explained.

Starting from the first walking joint, it performs a forward displacement (θ_{b1}) of the rover body around the first wheel. The displacement is carried out by the action of the walking motor torque (τ_{b1}) that also causes a contrary inertial force in the XZ axis that depends on the mass of the rover body m_b. Moreover, the effect of the gravity g may be taken into account. So, using the d'Alembert principle [12], dynamics of this movement can be expressed as:

$$\sum T = \tau_{b1} - B_m \cdot \dot{\theta}_{b1} - J_m \cdot \ddot{\theta}_{b1} - \frac{m_b}{n/2} \cdot \ddot{x}_b \cdot l \cdot cos(\theta_{b1}) - \frac{m_b}{n} \cdot (\ddot{z}_b + g) \cdot l \cdot sin(\theta_{b1}) = 0 \tag{7}$$

where the first line represents the motor dynamics defined by the rotational damper B_m and the motor axis inertia J_m. The rest of terms represent the rover body dynamics due to the movement in the X and Z axis, translated into torques. Also, m_b is the the body mass that is divided by the number of wheels n, g is the gravity and l is the distance between the center of the body and wheel.

The wheel (x_{w1}, z_{w1}) is attached to a bar that is moved by the wheel-walking motor (τ_{b1}). This wheel performs a movement to keep it locked with respect to the terrain, i.e. the bar is moving as the walking motor. Dynamics of this movement can be expressed as:

$$\sum T = \tau_{w1} - B_m \cdot \dot{\theta}_{w1} - J_w \cdot \ddot{\theta}_{w1} \tag{8}$$

It is worth mentioning this wheel has a horizontal displacement due to the drawbar pull forces derived from the exerted torque τ_{b1}. This movement is carried out only when the drawbar pull force F_{dpw1} is higher than the friction force $\mu \cdot F_{Nw1}$. In this situation, dynamics of the movement can be expressed as:

$$\sum F = F_{dpw1} - m_w \cdot \ddot{x}_{w1} - sgn(\dot{x}_{w1}) \cdot \mu \cdot F_{Nw1} = 0 \tag{9}$$

where the drawbar pull force can be calcuated as:

$$F_{dpw1} = \frac{\tau_{b1}}{l} \cdot cos(\theta_{b1}) \tag{10}$$

and the normal force is:

$$F_{Nw1} = \frac{m_b}{n} \cdot g + \frac{\tau_{b1}}{l} \cdot sin(\theta_{b1}) \tag{11}$$

As regards the second walking joint (τ_{b2}, θ_{b2}), its objective is to keep the rover body centered and move forward the second wheel (x_{w2}, y_{w2}). For this purpose, the second walking motor performs forward displacement (θ_{b2}), which causes a contrary inertial force because of the forward movement of the wheel and the vertical movement of the rover body. Thus, dynamics can be expressed as:

$$\sum T = \tau_{b2} - B_m \cdot \dot{\theta}_{b2} - J_m \cdot \ddot{\theta}_{b2} - m_w \cdot l \cdot \ddot{x}_{w2} \cdot cos(\theta_{b2}) - \frac{m_b}{n}(\ddot{z}_b + g) \cdot l \cdot sin(\theta_{b2}) = 0 \tag{12}$$

where m_w is the wheel mass. Moreover, the movement of this joint generates a drawbar pull force F_{dpw2} that is defined as:

$$F_{dpw2} = \frac{\tau_{b2}}{l} \cdot cos(\theta_{b2}) \tag{13}$$

Finally, the wheel in (x_{w2}, y_{w2}) has a motor that provides a torque τ_{w2} and it is also affected by the drawbar pull force

F_{dpw2} (13) and the wheel friction as follows:

$$\sum T = \tau_{w2} + F_{dpw2} \cdot r - \\ - B_m \cdot \dot{\theta}_{w2} - (J_m + J_w) \cdot \ddot{\theta}_{w2} - \cancel{\mu \cdot F_{Nw2} \cdot r} = 0 \quad (14)$$

where J_w represents the moment of inertia of the wheel. In the case of this wheel, to avoid slip, it rolls at the same velocity as it is moving because of the displacement in θ_{b2}. Therefore, taking into account experimental results from [10], it can be assumed the friction coefficient is null ($\mu \approx 0$) if there is no slip ($s \approx 0$), therefore, the last term of (14) can be removed.

B. Normal driving

The *normal driving* locomotion mode represents the walking joints locked in a vertical position and a wheel rolling by the action of a torque (τ) that is generated by a motor. It is assumed there is no generated torque from the walking joints, i.e. $\tau_{b1} = 0$ and $\tau_{b2} = 0$ e.g. these joint are provided with an electrical brake. Taking into account the wheel slip (s) (2) when it is rolling, the transmitted drawbar pull force (F_{dp}) from a wheel (τ,θ) to the rover body can be expressed as:

$$F_{dp} = (1 - s) \cdot \frac{\tau}{r} \quad (15)$$

Relation between the angular rotation of the wheel (θ) and the traversed distance (x) by the rover can be expressed as:

$$x = \theta \cdot r \cdot (1 - s) \quad (16)$$

Therefore, translating the wheel–body dynamics into torques, and using again the d'Alembert principle, equation that represents the rover movement can be defined as:

$$\sum T = \tau \cdot (1 - s) - \left(\frac{J_w}{r} + \frac{m_b}{n} \cdot r \right) \cdot \ddot{x} - \frac{B_t}{r} \cdot \dot{x} \\ - \mu \cdot F_N \cdot r = 0 \quad (17)$$

where $F_N = (m_b/n) \cdot g$ is the normal force exerted by the wheel over the terrain because of the action of gravity.

C. Electrical power consumption

Each locomotion mode consumes more or less electrical energy to advance depending on the terrain features. Therefore, the parameter P is introduced as the power required to traverse a terrain at a certain velocity depending on μ and s. Assuming the motors are linear, this parameter is proportional to the sum of the motor torques. In the case of the driving mode, P is obtained through (18). On the other hand, although in wheel-walking such sum of torques is not constant along the time, an equivalent constant power can be obtained integrating all torques during an entire stride and dividing the result by the elapsed time Δt (19).

$$P_d = \sum_{i=1}^{n} \frac{V_i}{K_{Ti} \cdot R_i} |\tau_i| \quad (18)$$

$$P_{ww} = \frac{V_i}{\Delta t} \sum_{i=1}^{2n} \int_{\Delta t} \frac{1}{K_{Ti} \cdot R_i} |\tau_i| \, dt \quad (19)$$

In these equations, K_{Ti} is the motor torque constant, V_i the voltage supplied, R_i the gear ratio for the i joint and n the total number of wheels.
Summarizing this section, two locomotion modes have been modeled taking into account the slip ration and dynamic friction coefficient. It will allow to perform several simulations with the aim of estimating the energy required for each locomotion mode depending on these parameters. Results of these simulations will be used in next section to perform a path planning, able to choose between both locomotion modes.

III. PATH PLANNING

This section details the proposed path planning algorithm, whose main objective is to find the optimal path for arriving at a desired destination with the least possible energy consumed, taking into consideration the two modeled locomotion modes.

First, the surface on which the path planning operates is discretized into a mesh. It consists on a square grid where the intersection of its lines are called nodes. Each node N_{ij}, where i and j are the coordinates that indicate its location on the grid, contains information about the features μ_{ij} and s_{ij} of the terrain on which it is placed.

The proposed path planning algorithm is based on the Fast Marching method. It consists on calculating the expansion of a wave that starts from the initial point and propagates to the rest of nodes. As a result, a stationary potential field with no local minimal points is obtained, whose values indicate the minimum cost needed to arrive at each node. Previous contributions [9] and [13] considered this cost as the minimal arrival time. However, the proposed function cost provides information about the power consumption using both locomotion modes as explained below.

A. Cost Function

The amount of power required to arrive at a certain node N_{ij} is the *Work* (W_{ij}) the rover must generate. It is calculated as the integration of P_{ij} with respect to the elapsed time. Therefore, the propagation wave at a rover constant velocity v_b can be calculated using the spatial derivative of W_{ij} as:

$$P_{ij} = \dot{W_{ij}} = ||\nabla W_{ij}|| v_b \quad , \quad ||\nabla W_{ij}|| = \frac{P_{ij}}{v_b} \quad (20)$$

where the last expression is the proposed Eikonal equation for the Fast Marching algorithm in terms of power consumption. As it is preferable to employ the least possible power, P_{ij} can be defined as:

$$P_{ij} = min(P_{ww}(\mu_{ij}, s_{ij}), P_d(\mu_{ij}, s_{ij})) \quad (21)$$

where P_{ww} and P_d are the power needed for each locomotion mode depending on the terrain features (μ and s) as defined in (18) and (19) respectively. It is worth mentioning the value of P_{ij}/v_b is always positive, so it is ensured that no local minimums are created in the resulting potential field.

B. Potential Field

The discretized expression of (20) to be used in the Fast Marching algorithm is the quadratic one presented in (22), where W_{ij} is calculated for each node N_{ij} and P_{ij} is obtained from (21). This expression ensures the resulting value of W_{ij} is a value higher than its respective neighbors. As this expression is used only once for each node, the resulting potential field is stationary. In this case, the parameters Δx and Δy are the horizontal and vertical distance between nodes respectively.

$$\left(\max\left\{\frac{W_{ij}-W_{i-1,j}}{\Delta x},\frac{W_{ij}-W_{i+1,j}}{\Delta x},0\right\}\right)^2+\left(\max\left\{\frac{W_{ij}-W_{i,j-1}}{\Delta y},\frac{W_{ij}-W_{i,j+1}}{\Delta y},0\right\}\right)^2=\left(\frac{P_{ij}}{v_b}\right)^2 \quad (22)$$

As result, a potential field is created containing the values of each W_{ij} node.

C. Final Path extraction

The final step is to get the path, composed by a set of waypoints $\Gamma(k)=(\Gamma_x,\Gamma_y)$ connecting the goal and starting positions, by applying a Gradient Descent Method. This method is implemented as follows: being K the total number of waypoints, which depends on a step parameter called γ (usually not larger than Δx and Δy) and having $\Gamma(0)$ as the start node and $\Gamma(K)$ as the goal node, the position of the rest of waypoints $\Gamma(1),\Gamma(2),...\Gamma(K-1)$ is determined using equations (23) and (24). First, the partial derivatives in x and y of W_{ij} are Gx_{ij} and Gy_{ij} respectively. Then, the value of such partial derivatives for a waypoint $\Gamma(k)$ is interpolated using its position (Γ_x,Γ_y), obtaining as result $Gx(\Gamma(k))$ and $Gy(\Gamma(k))$.

$$\Gamma_x(k-1)=\Gamma_x(k)-\gamma\cdot Gx(\Gamma(k)) \quad (23)$$

$$\Gamma_y(k-1)=\Gamma_y(k)-\gamma\cdot Gy(\Gamma(k)) \quad (24)$$

To determine the locomotion mode chosen to arrive at each waypoint $\Gamma(k)$ a matrix L is created to indicate such mode with a binary value according to equation (25).

$$L_{ij}=\begin{cases}0\ ,\ P_{i,j}=P_d(\mu_{ij},s_{ij})\\ 1\ ,\ P_{i,j}=P_{ww}(\mu_{ij},s_{ij})\end{cases} \quad (25)$$

Interpolating each waypoint in the L matrix built from equation (25) using its position gives a result rounded to 0 (normal driving) or 1 (wheel-walking).

To sum up, a fast marching algorithm has been used with an Eikonal equation defined in terms of power consumption, and a cost function that takes into account both locomotion modes and its dependency with wheel-soil interaction parameters μ and s. As result, a smooth and continuous optimal trajectory is obtained, taking advantage of the dynamics models of both locomotion modes for different terrains.

TABLE I: Simulation values

Parameter	Value	Unit	Parameter	Value	Unit
B_m	$11\cdot10^{-5}$	Nms/rad	g	3.711	m/s^2
J_m	$4.36\cdot10^{-7}$	$kg\,m^2$	r	0.07	m
J_w	$12\cdot10^{-4}$	$kg\,m^2$	v_b	0.02	m/s
l	0.125	m	n	6	–
m_b	15	kg	$R_{1,2,3}$	$1:19$	–
m_w	0.484	kg	$K_{T_{1,2,3}}$	$10,9$	mNm/A

IV. SIMULATION

To demonstrate the rover locomotion models and how they are used to decide between them in the proposed path planning algorithm, two different simulations were carried out. First, both locomotion modes were simulated to obtain the power consumption in terms of friction and slip ratio. Afterwards, these results were used to calculate a path in an area where both locomotion modes improved the power consumption.

A. Locomotion modes

Simulation of both locomotion modes were carried out using the ExoTeR [5] rover parameters (Table I). This rover belongs to the European Space Agency and the aim is to validate obtained results with it in the future. Equations (1)-(19) were implemented in *Matlab-Simulink*. Rover speed was fixed to 2 cm/s for both locomotion modes. As regards the wheel-walking, initial and final step angles were the same as used in previous experiments using the ExoTeR rover [5]: $-15^o\leq\theta_{1,2}\leq15^o$.

Several simulations were performed using different values of friction and slip ratio (Figure 2) using *wheel-walking* (blue) and *normal driving* (green). As can be appreciated, the wheel-walking power consumption keeps almost constant ($Power\approx0.2kW$) for different values of friction and slip. It is because this locomotion mode is only affected by the

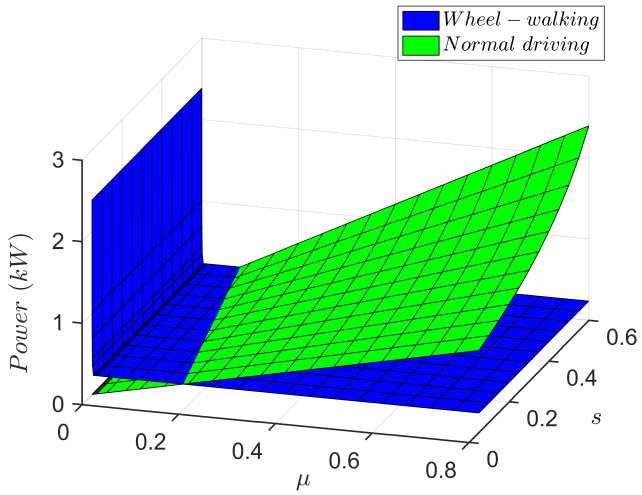

Fig. 2: Instant power consumption by the ExoTeR rover for each locomotion mode according to the values of slip ratio and dynamic friction coefficient.

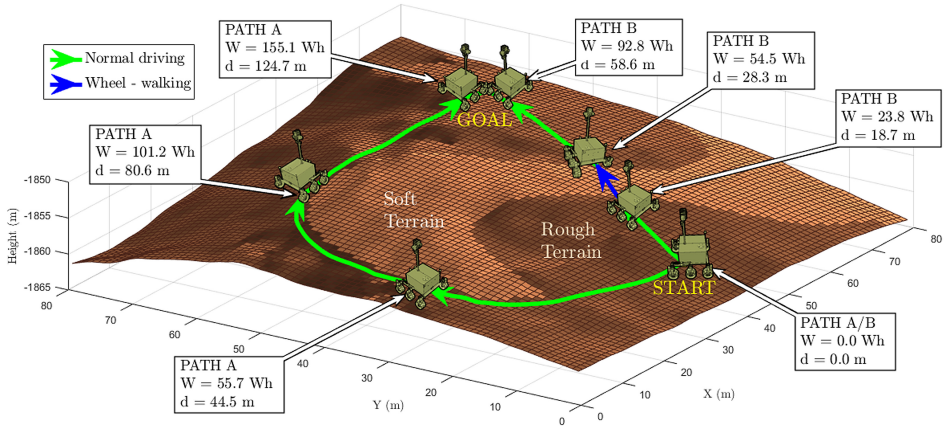

Fig. 3: Optimal paths using one locomotion mode (Path A) and both of them (Path B). Green and blue lines represent normal driving and wheel-walking respectively. Total traverse distance and electrical power consumption are also represented for different waypoints.

friction. One wheel does not roll, which means it is only affected by the friction, and the other one rolls at the same velocity as it is moved by the walking motor, i.e. there is no slip. Comparing both locomotion modes, there are an interval in which the wheel-walking power consumption is lower than using normal driving. In particular, wheel-walking is the best choice if there is a high friction coefficient and slip ratio, e.g. soft terrains as dunes or similar. However, normal driving improves the power consumption in terrains with low friction coefficient and slip ratio ($\mu \leq 0.15$), e.g. rough terrains. Moreover, when the friction coefficient is too low ($\mu \leq 0.05$), power consumption in wheel-walking tends to infinite because of the wheel sliding, e.g. rover on ice. Finally, maximum motors power should be taken into account because they could saturate and do not reach the required power.

B. Path planning

A customized simulation environment was used to test the performance of the implemented path planning algorithm. It is composed of a ROS architecture that connects several nodes, each one responsible of various control layers to command the rover. One of these nodes is the responsible of the implementation of the proposed Fast Marching algorithm. On the other hand, a ROS node is connected to the V-REP simulation software, which uses Vortex as its Object Dynamics Engine (ODE). So, a virtual Martian scene and the ExoteR rover were integrated within the simulation environment. Such scene was created using a DEM obtained from HiRISE. This repository provides high resolution images from the surface of Mars using a camera system [14]. A 80x80m DEM showing the peak of the Husband Hill was extracted from [15]. This place is interesting because it is situated in Gusev Crater, which was traversed once by the Spirit rover.

With the aim of testing the rover performance in different terrains, in which the use of both locomotion modes may be mandatory, the scene presents two types of terrain, soft and rough. Parameters of these terrains have been fixed from Table II. The soft terrain is distributed along the surface with the form of a hook as shown in Figure 3. The rover determines the value of these parameters from a matrix given beforehand, where each element indicates the terrain parameters (μ and s) for each node in the grid, as explained in Section III. An example of the estimation of these parameters in a real world is explained in [11], where it used a vision-based classifier.

The test consisted on going from a starting position to a goal position in the scene, finding the optimal path considering terrain features and the available locomotion modes. The simulation was run twice considering two cases: the first one with only the normal driving locomotion mode (Path A); and the second one where the rover was able to use both locomotion modes (Path B), as shown in Figure 3.

Figure 4 shows the potential fields of W using the Fast Marching algorithm for the two previously defined cases: Path A and B. In Figure 4.a can be clearly appreciated how the planned path avoids an area with high power consumption using only normal driving. Conversely, figure 4.b shows how the use of wheel-walking allows finding a path whose cost is lower than the previous case (92.8 Wh for path B and 155.1 Wh for path A).

At last, a demonstration video is attached to this paper. It shows the developed simulation environment in V-REP software. First, a goal position is chosen. Later on, the optimal path plan is calculated using the described method and models, and finally, the path is performed by the ExoTeR rover.

TABLE II: Terrain parameters

Terrain model	μ	s	$P_{ww}\,(kW)$	$P_d\,(kW)$
Rough	0.07	0.05	0.236	0.088
Soft	0.45	0.5	0.236	1.074

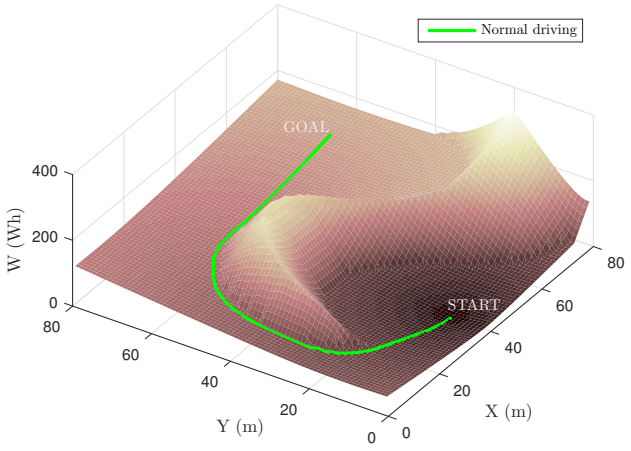

(a) Only driving mode (Path A)

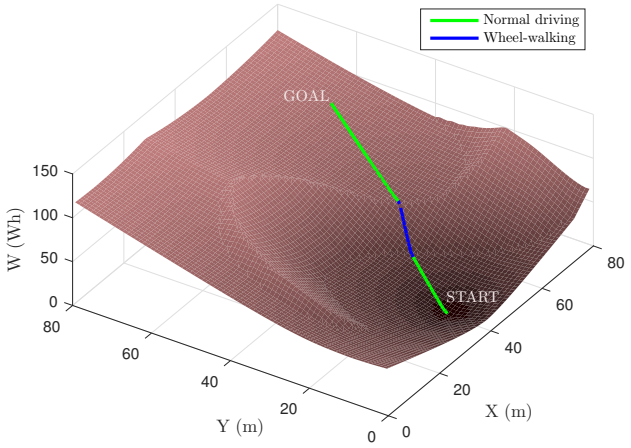

(b) Driving and wheel-walking modes (Path B)

Fig. 4: Potential Fields of W obtained when using only normal driving (a) or both driving and wheel-walking (b). Lighter colors on the surface represents a higher cost.

V. CONCLUSIONS

This paper proposes dynamics models for two locomotion modes with the aim of demonstrate which one is the best, in terms of power consumption, depending on the terrain features. Result of simulations, for a particular rover (ExoTeR), shows that a low friction coefficient and slip ratio recommends the use of a normal driving locomotion. However, if the friction coefficient and slip ratio get increased, wheel-walking consumes less power than driving. The choice between both locomotion modes is determined by the rover dynamics configuration.

On the other hand, a path planning algorithm, based on Fast Marching, has been used to generate a path that takes into account both locomotion modes and the best one depending on the terrain features. Performed simulations show there are some cases in which it would better to use a less efficient locomotion mode in order to traverse a shorter distance, and therefore, improve the total power consumption during the path.

Finally, dynamics models would be extended to take into account more parameters related to the rover and terrain features. Moreover, defined models should be compared with obtained measurements from the real rover ExoTeR. On the other hand, although the proposed path planning algorithm has demonstrated promising results for both locomotion modes, it would be extended to take into account more parameters in the function cost, e.g. hazards, solar radiation exposure, etc. These issues are proposed as future works.

REFERENCES

[1] Ajey Lele. Mars missions: Past, present and future. In *Mission Mars*, pages 85–92. Springer, 2014.

[2] Mark Woods, Andy Shaw, Dave Barnes, Dave Price, Derek Long, and Derek Pullan. Autonomous science for an exomars rover–like mission. *Journal of Field Robotics*, 26(4):358–390, 2009.

[3] Nildeep Patel, Richard Slade, and Jim Clemmet. The exomars rover locomotion subsystem. *Journal of Terramechanics*, 47(4):227–242, 2010.

[4] Marcus Y Woo. Roving on mars. *Engineering and Science*, 72(2):12–20, 2009.

[5] Martin Azkarate, Martin Zwick, Javier Hidalgo-Carrio, Robin Nelen, Tim Wiese, Pantelis Poulakis, Luc Joudrier, and Gianfranco Visentin. First experimental investigations on wheel-walking for improving triple-bogie rover locomotion performances. In *13th Symposium on Advanced Space Technologies in Robotics and Automation*, pages 1–6. ESA, 2015.

[6] Scott Moreland, Krzysztof Skonieczny, David Wettergreen, Vivake Asnani, Colin Creager, and Heather Oravec. Inching locomotion for planetary rover mobility. In *Aerospace Conference, 2011 IEEE*, pages 1–6. IEEE, 2011.

[7] Masataku Sutoh, Junya Yusa, Tsuyoshi Ito, Keiji Nagatani, and Kazuya Yoshida. Traveling performance evaluation of planetary rovers on loose soil. *Journal of Field Robotics*, 29(4):648–662, 2012.

[8] Eric Rohmer, Giulio Reina, and Kazuya Yoshida. Dynamic simulation-based action planner for a reconfigurable hybrid leg–wheel planetary exploration rover. *Advanced Robotics*, 24(8-9):1219–1238, 2010.

[9] Santiago Garrido, María Malfaz, and Dolores Blanco. Application of the fast marching method for outdoor motion planning in robotics. *Robotics and Autonomous Systems*, 61(2):106–114, 2013.

[10] Carlos Canudas-de Wit, Panagiotis Tsiotras, Efstathios Velenis, Michel Basset, and Gerard Gissinger. Dynamic friction models for road/tire longitudinal interaction. *Vehicle System Dynamics*, 39(3):189–226, 2003.

[11] Christopher A Brooks and Karl Iagnemma. Self-supervised terrain classification for planetary surface exploration rovers. *Journal of Field Robotics*, 29(3):445–468, 2012.

[12] Javier Fernandez De Canete, Cipriano Galindo, and Inmaculada Garcia-Moral. *System Engineering and Automation: An Interactive Educational Approach*. Springer Science & Business Media, 2011.

[13] Clement Petres, Yan Pailhas, Yvan Petillot, and Dave Lane. Underwater path planing using fast marching algorithms. In *Oceans 2005-Europe*, volume 2, pages 814–819. IEEE, 2005.

[14] Alfred S McEwen, Eric M Eliason, James W Bergstrom, Nathan T Bridges, Candice J Hansen, W Alan Delamere, John A Grant, Virginia C Gulick, Kenneth E Herkenhoff, Laszlo Keszthelyi, et al. Mars reconnaissance orbiter's high resolution imaging science experiment (hirise). *Journal of Geophysical Research: Planets*, 112(E5), 2007.

[15] Steve Squyres. Mars Exploration Rover Spirit Landing Site at Gusev Crater. `http://www.uahirise.org/PSP_001513_1655`, 2006. [Online; accessed 28-January-2017].